Effect of pulse depletion in a Brillouin optical time-domain analysis system

Luc Thévenaz,[1*] Stella Foaleng Mafang[1] and Jie Lin[1,2]

[1]*EPFL Swiss Federal Institute of Technology, Group for Fibre Optics, Institute of Electrical Engineering, SCI-STI-LT Station11, CH-1015 Lausanne, Switzerland*

[2]*Permanent address: Department of Electrical Engineering, Bucknell University, Lewisburg, PA 17837 USA*

**Luc.Thevenaz@EPFL.CH*

Abstract: Energy transfer between the interacting waves in a distributed Brillouin sensor can result in a distorted measurement of the local Brillouin gain spectrum, leading to systematic errors. It is demonstrated that this depletion effect can be precisely modelled. This has been validated by experimental tests in an excellent quantitative agreement. Strict guidelines can be enunciated from the model to make the impact of depletion negligible, for any type and any length of fiber.

OCIS codes: (060.2310) Fiber optics; (060.2370) Fiber optics sensors; (290.5900) Scattering, stimulated Brillouin; (060.4370) Nonlinear optics, fibers.

References and links

1. L. Thévenaz, "Brillouin distributed time-domain sensing in optical fibers: state of the art and perspectives," Front. Optoelectron. China **3**(1), 13–21 (2010).
2. M. A. Soto, G. Bolognini, F. Di Pasquale, and L. Thévenaz, "Long-range Brillouin optical time-domain analysis sensor employing pulse coding techniques," Meas. Sci. Technol. **21**(9), 094024 (2010).
3. M. A. Soto, M. Taki, G. Bolognini, and F. D. Pasquale, "Simplex-coded BOTDA sensor over 120-km SMF with 1-m spatial resolution assisted by optimized bidirectional Raman amplification," IEEE Photon. Technol. Lett. **24**(20), 1823–1826 (2012).
4. X. Angulo-Vinuesa, S. Martin-Lopez, J. Nuno, P. Corredera, J. D. Ania-Castanon, L. Thevenaz, and M. Gonzalez-Herraez, "Raman-assisted Brillouin distributed temperature sensor over 100 km featuring 2 meter resolution and 1.2°C uncertainty," J. Lightwave Technol. **30**(8), 1060–1065 (2012).
5. A. Fellay, L. Thévenaz, M. Facchini, and P. A. Robert, "Limitation of Brillouin time-domain analysis by Raman scattering," in *5th Optical Fibre Measurement Conference*, (Université de Nantes, 1999), 110–113.
6. S. M. Foaleng and L. Thevenaz, "Impact of Raman scattering and modulation instability on the performances of Brillouin sensors," Proc. SPIE **7753**, 77539V1–77539V-4 (2011).
7. M. N. Alahbabi, Y. T. Cho, T. P. Newson, P. C. Wait, and A. H. Hartog, "Influence of modulation instability on distributed optical fiber sensors based on spontaneous Brillouin scattering," J. Opt. Soc. Am. B **21**(6), 1156–1160 (2004).
8. D. Alasia, M. Gonzalez Herraez, L. Abrardi, S. Martin-Lopez, and L. Thevenaz, "Detrimental effect of modulation instability on distributed optical fiber sensors using stimulated Brillouin scattering," Proc. SPIE **5855**, 587–590 (2005).
9. T. Horiguchi, K. Shimizu, T. Kurashima, M. Tateda, and Y. Koyamada, "Development of a distributed sensing technique using Brillouin scattering," J. Lightwave Technol. **13**(7), 1296–1302 (1995).
10. E. Geinitz, S. Jetschke, U. Röpke, S. Schröter, R. Willsch, and H. Bartelt, "The influence of pulse amplification on distributed fibre-optic Brillouin sensing and a method to compensate for systematic errors," Meas. Sci. Technol. **10**(2), 112–116 (1999).
11. A. Minardo, R. Bernini, L. Zeni, L. Thevenaz, and F. Briffod, "A reconstruction technique for long-range stimulated Brillouin scattering distributed fibre-optic sensors: Experimental results," Meas. Sci. Technol. **16**(4), 900–908 (2005).
12. S. Martin-Lopez, M. Alcon-Camas, F. Rodriguez, P. Corredera, J. D. Ania-Castañon, L. Thévenaz, and M. Gonzalez-Herraez, "Brillouin optical time-domain analysis assisted by second-order Raman amplification," Opt. Express **18**(18), 18769–18778 (2010).
13. Y. Dong, L. Chen, and X. Bao, "System optimization of a long-range Brillouin-loss-based distributed fiber sensor," Appl. Opt. **49**(27), 5020–5025 (2010).
14. M. Niklès, L. Thévenaz, and P. A. Robert, "Simple distributed fiber sensor based on Brillouin gain spectrum analysis," Opt. Lett. **21**(10), 758–760 (1996).
15. S. Diaz, S. Mafang-Foaleng, M. Lopez-Amo, and L. Thevenaz, "A high-performance optical time-domain Brillouin distributed fiber sensor," IEEE Sens. J. **8**(7), 1268–1272 (2008).

#188493 - $15.00 USD Received 8 Apr 2013; revised 25 May 2013; accepted 27 May 2013; published 4 Jun 2013

16. A. Minardo, R. Bernini, and L. Zeni, "A simple technique for reducing pump depletion in long-range distributed Brillouin fiber sensors," IEEE Sens. J. **9**(6), 633–634 (2009).
17. R. Bernini, A. Minardo, and L. Zeni, "Long-range distributed Brillouin fiber sensors by use of an unbalanced double sideband probe," Opt. Express **19**(24), 23845–23856 (2011).
18. Y. Dong, X. Bao, and L. Chen, "High performance Brillouin strain and temperature sensor based on frequency division multiplexing using nonuniform fibers over 75km fiber," Proc. SPIE **7753**, 77533H1–77533H-4 (2011).
19. A. Zornoza, A. Minardo, R. Bernini, A. Loayssa, and L. Zeni, "Pulsing the probe wave to reduce nonlocal effects in Brillouin optical time-domain analysis (BOTDA) sensors," IEEE Sens. J. **11**(4), 1067–1068 (2011).
20. Y. Dong, L. Chen, and X. Bao, "Time-division multiplexing-based BOTDA over 100 km sensing length," Opt. Lett. **36**(2), 277–279 (2011).

1. Introduction

Distributed Brillouin fiber sensors have been widely employed for various physical sensing applications such as temperature and strain measurements in various infrastructures. They have become the most favorable and prominent fiber sensing system, with recent progresses towards centimeter spatial resolution [1] and over an extended distance range reaching 100 km recently [2–4]. Effects having a negligible impact on short distances build up and become extremely detrimental over an extended distance range. Among these effects, the spectral transfers due to stimulated Raman scattering [5, 6] and modulation instability [7, 8] were identified and studied several years ago. These two effects lead to a total extinction of the pump wave and a sharp drop of the Brillouin gain after a critical distance directly scaled by the peak pump power. A third effect, resulting from the gradual power transfer from the higher frequency wave to the lower frequency wave, has not been considered as a major concern so far, since it is more insidious and does not impair the basic operation of the sensor. The detrimental impact of this effect has nevertheless been mentioned at an early stage during the development of Brillouin fiber sensing techniques [9, 10]. As a result of the increasing range and accuracy, there have been recently some reports that focus on this effect by proposing a correction procedure based on an algorithm [11], by explicitly checking its absence of negative impact through a proper scaling of the signal powers [2, 12], or by showing and evaluating its biasing effect experimentally [13]. At the present stage, these studies are not fully completed to provide the proper guidance for a robust sensor design minimizing the depletion effect and to give the expressions that enable a quantitative evaluation of the impact of depletion on the sensor accuracy.

In this paper, a complete model that addresses the detrimental impact of the power transfer between the pump pulse and the probe signal in the case of a Brillouin Optical Time Domain Analysis (BOTDA) sensor is developed on the basis of the pioneering work [9, 10]. In the situation addressed by the model, a pump pulse and a probe CW signal counterpropagate in the fiber, corresponding to the vast majority of time-domain based Brillouin sensors. As suggested by a simple physical intuition, the amplitude of the pump pulse depends on the pump-probe frequency difference in presence of a substantial cumulated energy transfer between the 2 interacting waves. It must be immediately pointed out that the impact will be much bigger on the pump pulse, which continuously interacts with the CW probe all along the fiber, than on the probe signal, for which each time-resolved segment only interacts with the pump over a restricted length determined by the pulse duration. Since this energy transfer is distributed all along the fiber and is cumulative for the pump pulse, the effect will be much more severe when the pulse approaches the far end of the fiber. In other words, the conservation of energy requires that the total energy gained by one wave is equal to the total energy lost by the other wave. However, since this total energy transfer for the CW probe signal is distributed over the total propagation time through the fiber, the probe signal power change is much smaller than that of the pump pulse, for which the total energy transfer occurs

#188493 - $15.00 USD Received 8 Apr 2013; revised 25 May 2013; accepted 27 May 2013; published 4 Jun 2013

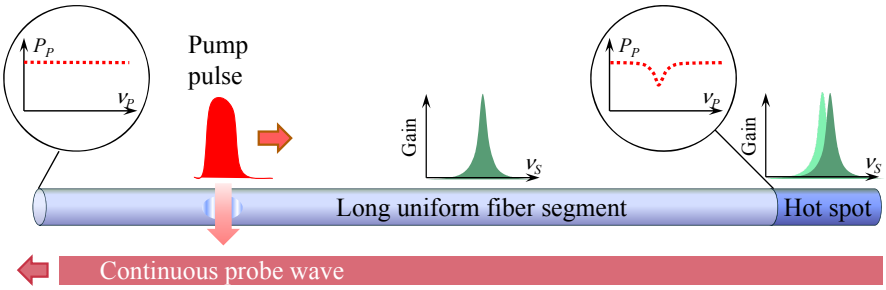

Fig. 1. Situation maximizing the impact of depletion (worst case situation): the pump pulse gradually transfers a fraction of its power to the continuous probe wave through the intercession of the acoustic wave created by the stimulated Brillouin scattering process. The Brillouin gain distribution is analyzed by scanning the pump-probe frequency difference and the pump pulse power is the same at the fiber input for any frequency difference, as shown in the left circle. If the Brillouin gain spectrum is uniform along most of the initial section of the fiber, the gradual power transfer between pump and probe is maximized at the peak gain frequency and non-uniform pump pulse power as a function of the frequency difference can result from this gradual depletion at the end of this uniform segment, as shown on the right circle. If a following fiber section with a slightly shifted gain spectrum is present, it is analyzed with a non-constant pump power for all frequencies and the measured gain spectrum of this section is distorted.

only during the pulse duration. The estimated factor in the difference of the power change experienced by the two signals can be as high as 1000 in a kilometer-long sensor with a meter spatial resolution.

Since the sensor response is essentially driven by this energy transfer, variations of the pulse amplitude at the fiber far end can be never avoided practically. The objective of this paper is to give limits and guidelines in making the power variations sufficiently negligible to ensure a preset accuracy on the determination of the Brillouin frequency. The practical impact is observed as uncontrolled amplitude change of the pump pulse after some distance along the fiber: the pulse amplitude will depend on the cumulative history of the stimulated Brillouin scattering energy transfer from the fiber input to the distant observation point. The change will be a function of the cumulative interaction strength along the fiber, so essentially of the pump-probe frequency difference and of the originally unpredictable longitudinal distribution of the Brillouin frequency. The result is a pump pulse power that cannot be certified to be constant when the pump-probe frequency difference is scanned. The Brillouin frequency response at a given position can therefore be analyzed with an activating signal showing a frequency-dependent power and a distorted gain spectrum can be consequently observed. The frequency dependency is of larger importance in the case of a uniformly distributed Brillouin spectrum along the fiber, since the cumulative gain is maximized when the frequency difference between the pump and the probe exactly matches the Brillouin shift.

The frequency-dependent pump power will provide a biased measurement of the gain spectral distribution if the pump pulse enters a section in which the Brillouin gain central frequency is shifted with respect to the gain spectrum in the long uniform preceding section. This situation is depicted in Fig. 1 and represents the worst case, which is unlikely to be exactly reproduced in a real implementation. The worst case practically defines the upper limit of the biasing effect. In all other situations showing a non-uniform distribution of the Brillouin frequency the biasing effect would be alleviated since the pump power frequency dependence is spectrally better evened out. The here presented model is based on this worst case situation and provides quantitative evaluation of the systematic error on the peak gain frequency in a given experimental configuration. It also defines the condition leading to the maximal error. In addition, this model reveals the tolerable power transfer for a given maximum error and the power limits for interacting signals to ensure this given accuracy.

#188493 - $15.00 USD Received 8 Apr 2013; revised 25 May 2013; accepted 27 May 2013; published 4 Jun 2013

Finally the model is challenged by comparing its predictions with experimental results in a real BOTDA sensor and achieves an excellent agreement.

2. Model for the evaluation of the error due to pump depletion

As commonly defined the fiber sensor is in a gain configuration if the pump pulse frequency is higher than the probe signal frequency, otherwise it is in a loss configuration. It must be pointed out that both the gain and the loss configurations lead to an equally distorted measured gain spectrum, so that at first glance none of these configurations offers a decisive advantage. As it will be demonstrated hereafter this conclusion turns out to be fully supported by the results of our model, so we first address the case of a gain configuration without loss of generality, and then the model will naturally extend to both gain and loss configurations simply by a proper choice of the sign of the gain coefficient.

Starting in the case of a gain configuration and in the worst case situation depicted in Fig. 1, the power transfers from the pump pulse to the probe signal will be hereafter designated as pump depletion. The pump pulse is chosen to be launched at the near end of the fiber ($z = 0$), while the CW probe signal enters at the far end ($z = L$), as sketched in Fig. 1. The pump pulse will be gradually depleted by the continuous probe after propagating along the long uniform fiber, eventually causing a drop in the pump power when the frequency difference between the pump and the probe closely matches the Brillouin shift, as depicted in Fig. 1. The amount of depletion can be characterized by a dimensionless coefficient d:

$$d = (P_{Po} - P_P) / P_{Po} \tag{1}$$

where P_{Po} is the pump power in the absence of Brillouin interaction (no gain or no probe wave), and P_P is the pump power in the presence of the maximum interaction at the Brillouin peak gain frequency of the long uniform section. Note that the effect on the pump in a loss configuration can be identically represented by opting for a negative value of the coefficient d.

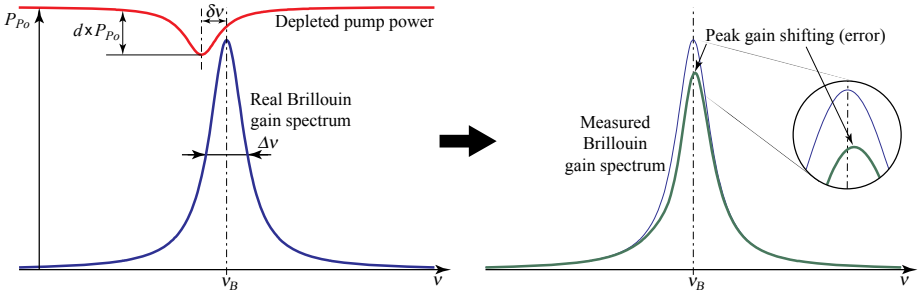

Fig. 2. Effect of a non-uniform frequency distribution of the pump pulse power on the measurement of the Brillouin gain spectrum: if the pump power is reduced by a fraction d at a given frequency and a Brillouin gain spectrum is analyzed with a peak gain frequency shifted by $\delta\nu$ from this given frequency, a distorted Brillouin gain spectrum will be measured, as shown on the right (thick solid line). The measured peak gain frequency is shifted with respect to the real gain spectrum (thin solid line) and suffers from a systematic error.

Now when this spectrally uneven pump power is used to analyze a distant fiber segment (highlighted in dark blue in Fig. 1), in which the Brillouin gain spectrum is slightly shifted by a frequency $\delta\nu$ with respect to the long preceding uniform section, the situation is like depicted in Fig. 2. The actual measured gain spectrum shows some asymmetric distortion, resulting in a shifted peak value and leading to a systematic error ν_e in the determination of the real maximum Brillouin gain frequency. It must be noted that the systematic error vanishes in 2 situations: 1) when the Brillouin gain spectrum in the distant segment shows no overlap with the dip present in the pump power frequency dependence, i.e. when the 2

#188493 - $15.00 USD Received 8 Apr 2013; revised 25 May 2013; accepted 27 May 2013; published 4 Jun 2013

sections are under very different environmental conditions; 2) when the 2 sections present the same Brillouin shift, resulting in a symmetric distortion of the measured gain spectrum that nullifies the systematic error. This error will therefore be maximized for a particular frequency difference $\delta\nu$ between the Brillouin shifts in the 2 sections, which will be determined by the model.

The full description of the effect of depletion on the sensor response requires 2 distinct stages that will be addressed successively hereafter:

1. For a given tolerable systematic error ν_e on the measured value of the maximum Brillouin gain frequency, determination of the maximum acceptable depletion coefficient d, assuming a perfectly Lorentzian distribution of the original Brillouin gain spectrum.

2. Determination of the relation between the pump pulse input power P_P, the CW signal input power P_S and the depletion coefficient d in the worst case depicted in Fig. 1, for given fiber characteristics and length.

Considering a high performance configuration with good spatial resolution, this model is based on the assumption that the gain or loss experienced by the probe signal during its brief local interaction with the pump pulse is very small and does not exceed at most a few percent (<5%). This is the typical case of all long range sensors showing a spatial resolution shorter than 2 meters. For higher gains the quantitative predictions may be less accurate.

2.1. Determination of the tolerable depletion d for a given error ν_e

Let's consider the Brillouin gain spectrum in the short section at the far end of the fiber to be:

$$g(\nu') = g_B \frac{1}{1+\left[\left(\nu'-\nu_B\right)/\Delta\nu/2\right]^2} \tag{2}$$

where ν' is the frequency difference between pump and probe, ν_B is the Brillouin shift corresponding to the maximal gain in the short section, and $\Delta\nu$ is the FWHM width of this gain spectrum. To simplify the expressions, the frequency origin is shifted to $\nu = \nu' - \nu_B$, (maximum gain at the frequency origin) without loss of generality.

If the maximal Brillouin gain frequency in the long uniform segment is shifted by $\delta\nu$ and the FWHM width $\Delta\nu$ is identical to the short segment, it is reasonable to assume that the short segment is made either of the same fiber or of at least a fairly identical one. The pump intensity follows this distribution:

$$I_P(\nu) = I_{Po}\, \mathrm{e}^{-\frac{d}{1+\left(\frac{\nu-\delta\nu}{\Delta\nu/2}\right)^2}} \approx I_{Po}\left[\ 1-\frac{d}{1+\left(\frac{\nu-\delta\nu}{\Delta\nu/2}\right)^2}\ \right] \tag{3}$$

where the linear approximation holds when the depletion is small (d<0.2), in which case it only results in a minor error on the pump power within 2% of its real value. This small depletion approximation is necessary to obtain expressions simple enough to lead to analytical solutions. It will be later checked that the tolerable depletion does not exceed 0.2 for standard acceptable systematic errors ν_e.

Having beforehand assumed a very small gain in the percent range experienced by the signal wave during its interaction with the pulse of duration T and propagating at the group velocity V_g, the net signal gain can be reasonably expressed by a first order expansion of the exponential amplification:

#188493 - $15.00 USD Received 8 Apr 2013; revised 25 May 2013; accepted 27 May 2013; published 4 Jun 2013

$$G(\nu) = e^{g(\nu)I_P(\nu)\frac{V_g T}{2}} \approx 1 + g(\nu)I_P(\nu)\frac{V_g T}{2} = 1 + g_B \frac{V_g T}{2} I_{Po} \frac{1}{1+\left(\frac{\nu}{\Delta\nu/2}\right)^2}\left[\, 1 - \frac{d}{1+\left(\frac{\nu-\delta\nu}{\Delta\nu/2}\right)^2} \,\right] \quad (4)$$

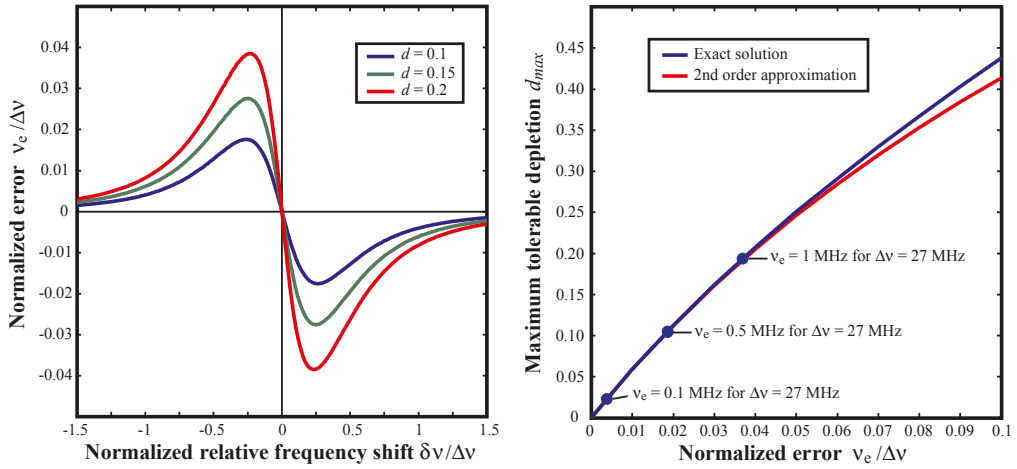

Fig. 3. Left: Systematic error normalized to the FWHM Brillouin gain linewidth, as a function of the normalized frequency shift between the gains in the long initial uniform segment and the local analyzed segment, for 3 different depletion factor *d*. The maximum error occurs when the 2 gain spectra are shifted by a quarter of linewidth. Right: Maximum tolerable depletion as a function of the maximum tolerable normalized error, in the situation of the relative frequency shift $\delta\nu$ leaving the maximum systematic error. The exact solution given by Eq. (8) is represented, as well as the 2nd order approximation given by Eq. (9). It shows that this approximation is excellent for depletion factors $d < 0.2$. Points for typical errors in standard G.652 fibers at a wavelength of 1550 nm are shown.

This distribution is shown on the right in Fig. 2 and presents a shifted maximum when compared to the distribution for $d = 0$. The amount of shifting depends on the magnitude of depletion d and on the relative shift $\delta\nu$ between the maximum gain frequencies of the two segments. The gain FWHM spectral width $\Delta\nu$ turns out to be a simple scaling factor, so that all results can actually be normalized to $\Delta\nu$. The error is found by searching the frequency ν giving the maximum gain in Eq. (4), by simply nulling the derivative of this expression.

The solution is one of the zeroes of a 5th degree polynomial expression from which no general solution can be easily extracted[6]:

$$\left(\frac{\nu_e}{\Delta\nu}\right)^5 - 4\left(\frac{\delta\nu}{\Delta\nu}\right)\left(\frac{\nu_e}{\Delta\nu}\right)^4 + \frac{1}{2}\left(12\left(\frac{\delta\nu}{\Delta\nu}\right)^2 + 1 - d\right)\left(\frac{\nu_e}{\Delta\nu}\right)^3 + \left(\frac{3}{4}d\left(\frac{\delta\nu}{\Delta\nu}\right) - 4\left(\frac{\delta\nu}{\Delta\nu}\right)^3 - \left(\frac{\delta\nu}{\Delta\nu}\right)\right)\left(\frac{\nu_e}{\Delta\nu}\right)^2 + \left(\left(\frac{\delta\nu}{\Delta\nu}\right)^4 + \frac{1}{4}(2-d)\left(\frac{\delta\nu}{\Delta\nu}\right)^2 + \frac{1}{16}(1-2d)\right)\left(\frac{\nu_e}{\Delta\nu}\right) + \frac{1}{16}d\left(\frac{\delta\nu}{\Delta\nu}\right) = 0 \quad (5)$$

A numerical solution can be found to illustrate the dependence. Figure 3 (left) shows the normalized error $\nu_e/\Delta\nu$ as a function of the normalized relative frequency shift $\delta\nu/\Delta\nu$ between the peak gains in the 2 sections, for 3 fixed depletion values d. The systematic error reaches its maximum value when the relative frequency shift is approximately 1/4 of the FWHM gain spectral width, while as expected it vanishes if there is no shift or a much larger shift than the gain spectral width (no overlap).

Given the effect of depletion is small, a first order solution for Eq. (5) can be obtained assuming that the error ν_e is much smaller than $\Delta\nu$:

#188493 - $15.00 USD Received 8 Apr 2013; revised 25 May 2013; accepted 27 May 2013; published 4 Jun 2013

$$\nu_e \cong -\frac{d\ \delta\nu}{\left(1+4\left(\frac{\delta\nu}{\Delta\nu}\right)^2\right)^2 - 2d\left(1+2\left(\frac{\delta\nu}{\Delta\nu}\right)^2\right)} \tag{6}$$

The global minus sign indicates that the maximum gain is logically shifted to higher frequencies when the long segment presents a peak gain at frequencies lower than that in the short segment (situation depicted in Fig. 1). For a fixed d, this expression is maximal when:

$$\delta\nu = \sqrt{\frac{2-d}{28}}\,\Delta\nu \approx 0.26\,\Delta\nu \quad \text{for a small depletion } d < 0.2. \tag{7}$$

Since d is a subtractive term on the plain number 2 and is assumed to be at least 10 times smaller, it has a small impact on the result and the rightmost approximate term in the expression is evaluated for the median value d = 0.1. This result shows that the error is maximal when the spectral shift between the peak gains in the two segments is about a quarter of the full width at half maximum, which is fully consistent with the graphical information shown in Fig. 3(left).

From a practical point of view it is essential to determine the tolerable amount of depletion d_{max} that would ensure an error not exceeding a given value ν_e. Inspecting Eq. (5) shows it is a linear function of the depletion factor d. An exact solution can be therefore obtained for d, assuming the approximation made to establish Eq. (4):

$$d_{\max} = \frac{-16e^5 + 64\xi e^4 - 8\left(12\xi^2+1\right)e^3 + \left(1+4\xi^2\right)\left[16\xi e^2 - \left(1+4\xi^2\right)e\right]}{-8e^3 + 12\xi e^2 - 2\left(1+2\xi^2\right)e + \xi} \tag{8}$$

$$\text{with } \xi = \frac{\delta\nu}{\Delta\nu} \text{ and } e = \frac{\nu_e}{\Delta\nu}.$$

Actually, considering that the systematic error ν_e is much smaller than the gain spectral width $\Delta\nu$ in a weak depletion regime, this expression can be simplified and a robust 2nd order approximate relation can be easily deduced:

$$d_{\max} = \frac{\left(1+4\xi^2\right)\left[16\xi e^2 - \left(1+4\xi^2\right)e\right]}{12\xi e^2 - 2\left(1+2\xi^2\right)e + \xi} \tag{9}$$

Figure 3 (right) shows the maximum tolerable depletion d_{max} for a given normalized error $\nu_e/\Delta\nu$ using Eq. (8) and (9), in the situation of the relative frequency shift $\delta\nu$ leaving the maximum systematic error as given by Eq. (7). Some important points are represented, corresponding to standard accuracies in Brillouin distributed sensors (1 MHz, 0.5 MHz, 0.1 MHz) using a gain FWHM spectral width of 27 MHz, which is a standard value according to our experience in the commonly used ITU-T G.652 fibers at a wavelength of 1550 nm. These standard accuracies require a maximum tolerable depletion of 0.194 for a maximum error of 1 MHz, while it must be reduced to 0.105 for an error of 0.5 MHz and to 0.023 for 0.1 MHz. This confirms the relevance of the approximation used for establishing the model (d<0.2) and its validity in real situations.

It must be mentioned that all results shown above equally apply to a loss configuration. In loss case a negative value for the depletion factor d has to be inserted in all expressions, leading to similar errors for small d. It should also be pointed out that depletion induces a distortion of the gain spectrum, which gives a biased evaluation of the peak gain frequency and thus leads to a systematic error that is not subject to statistical variations. When a sensing system is subject to depletion, the estimation of the accuracy calculated from the standard

#188493 - $15.00 USD Received 8 Apr 2013; revised 25 May 2013; accepted 27 May 2013; published 4 Jun 2013

deviation over repeated measurements does not actually inform on the real total error. Instead, the error can be increased by the systematic non-stochastic contribution due to depletion.

2.2. The 1st order maximum probe power in a gain configuration

Assuming the effect of the interaction has negligible impact on the global probe power P_S (small gain condition), the probe launched at the far end ($z = L$) will essentially experience an exponential decay due to the linear attenuation α, so that $P_S(z) = P_{iS}\, e^{-\alpha(L-z)}$ with $P_{iS} = P_S(L)$ the input signal power at the fiber far end. This is the assumption rooting the 1st order approximation. Then the pump power distribution $P_P(z)$ can be calculated by solving the basic equation for the Brillouin interaction, including the linear attenuation term:

$$dP_P = -\alpha P_P(z)\,dz - \frac{g_B}{A_{eff}} P_P(z)\,P_S(z)\,dz \tag{10}$$

where g_B and A_{eff} are the Brillouin linear gain and the nonlinear effective area of the propagating mode, respectively. It must be pointed out that g_B is considered here as position-independent, since the maximal depletion effect will be observed for the worst case scenario when the gain is maximal at any position and this is the situation addressed here.

An exact solution $P_P(z)$ can be found under the small gain assumption, given here by the following expression at $z = L$, for the residual output pump power $P_P(L)$ with the initial condition $P_{iP} = P_P(0)$:

$$P_P(L) = P_{iP}\, e^{-\alpha L}\, e^{-\frac{g_B}{\alpha A_{eff}} P_{iS}(1-e^{-\alpha L})} = P_{iP}\, e^{-\alpha L}\, e^{-\frac{g_B}{A_{eff}} P_{iS} L_{eff}} \quad \text{using} \quad L_{eff} = \frac{1-e^{-\alpha L}}{\alpha}. \tag{11}$$

The output pump power with a zero gain interaction simply reads $P_{Po}(L) = P_{iP}\, e^{-\alpha L}$, so that the depletion factor d can be easily derived from Eq. (1) and Eq. (11):

$$1-d = \frac{P_P(L)}{P_{Po}(L)} = e^{-\frac{g_B}{A_{eff}} P_{iS} L_{eff}} \tag{12}$$

Hence the maximum input probe signal power P_{iS} for a given tolerable depletion factor d can be expressed as:

$$P_{iS} < -\ln(1-d)\frac{A_{eff}}{g_B L_{eff}} \overset{L\to\infty}{=} -\ln(1-d)\frac{A_{eff}}{g_B}\alpha \tag{13}$$

This result shows that the maximum probe power P_{iS} is totally independent of the power P_P and the pulse width of the pump. For a given depletion factor d it solely depends on the fiber properties. This may hurt at first glance the good sense, but this is a direct consequence of the small gain approximation and the consecutive linear dependence between gain and pump power: the power transfer between pump and probe power is for sure larger for a higher pump power, but this power transfer scales in the exact same proportion as the pump power. The fractional depletion d is therefore independent of the pump power P_P and, as demonstrated in the previous sub-section, the systematic error ν_e is only function of d. In standard conditions ($g_B = 2 \times 10^{-11}$ m/W, $A_{eff} = 80 \times 10^{-12}$ m^2, $\alpha^{-1} = 22 \times 10^3$ m), for a depletion factor $d = 0.20$, the input probe power P_{iS} must not exceed 40 µW, which is a fairly low value, far from being respected by the vast majority – if not the entirety - of existing sensors.

Equation (13) can be rewritten differently to use more practical quantities, since the gain coefficient g_B and the effective mode area A_{eff} are practically difficult to evaluate. In a small gain situation, at the fiber input near end, the signal experiences the following gain G_i caused by the pump pulse (peak power P_{iP}, duration T):

#188493 - $15.00 USD Received 8 Apr 2013; revised 25 May 2013; accepted 27 May 2013; published 4 Jun 2013

$$G_i = \frac{g_B}{A_{eff}} P_{iP} \frac{V_g T}{2} \tag{14}$$

This gain G_i is easily observable and measurable on the signal waveform, so that the condition given by Eq. (13) can be rewritten as:

$$\frac{P_{iS}}{P_{iP}} < -\ln(1-d)\frac{V_g T}{2G_i L_{eff}} \overset{L\to\infty}{=\!=} -\ln(1-d)\frac{V_g T}{2G_i}\alpha \tag{15}$$

The small gain assumption stating that the probe power distribution along the fiber is essentially dictated by the linear loss can be invalidated in the reality, as a consequence of the finite extinction ratio of the unavoidably imperfect modulator shaping the pump pulse. In this situation a continuously pumping power leaks through the modulator and the probe will gradually experience a tiny amplification all along the fiber, which may eventually turn large once integrated all over the fiber length. A condition on the modulator extinction ratio can be deduced in this case, by assuming that the amplification resulting from this power leak gives no significant pump depletion. If depletion occurs, the integrated probe amplification is reduced, so that the result under this assumption can be securely considered as a worst case limit. By simply swapping the role of the 2 waves using the derivations in Eqs. (10)-(12) and by defining ξ as the on-off extinction ratio of the modulator, it can be straightforwardly deduced that the integrated probe amplification due to the modulator leak will be in the worst case:

$$G_\xi = \frac{g_B}{A_{eff}} \xi P_{iP} L_{eff}\,. \tag{16}$$

To arbitrarily set a limit, this amplification may be considered as having a negligible impact if it is smaller than the amplification experienced by the probe wave under the normal interaction with the pump pulse at the fiber input end:

$$\frac{g_B}{A_{eff}} \xi P_{iP} L_{eff} < \frac{g_B}{A_{eff}} P_{iP} \underbrace{\frac{V_g T}{2}}_{\Delta L} \tag{17}$$

where ΔL corresponds to the spatial resolution. After simplification this condition can be rewritten:

$$\xi < \frac{\Delta L}{L_{eff}} \tag{18}$$

For an asymptotically long fiber $L_{eff} = 22 \times 10^3$ m and a tight spatial resolution $\Delta L = 1$ m, the extinction ratio must be at least 43 dB to satisfy this condition. This is reduced to 36 dB for a spatial resolution $\Delta L = 5$ m. When the linear loss α can be neglected and $L_{eff} = L$, so typically for short fibers, the criterion simply reduces to the condition that the extinction ratio must be the exact inverse of the number of spatially resolved points $L / \Delta L$. By extension this can be considered as a general limit for modulator leaks in all Brillouin distributed sensing systems.

#188493 - $15.00 USD Received 8 Apr 2013; revised 25 May 2013; accepted 27 May 2013; published 4 Jun 2013

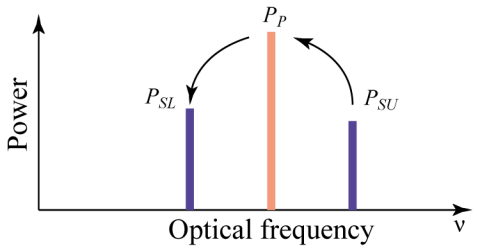

Fig. 4. General spectral arrangement of pump (P_P) and probe signals (P_{isL}, P_{isU}), including most practical situations in real Brillouin distributed sensors. The arrows indicate the directions of the power transfer due to the interaction and (signal in red propagates forwardly along the fiber, those in blue backwardly). The sensors may operate in gain regime (P_{isU} = 0), in loss regime (P_{isL} = 0) or in double-sideband configuration (P_{isU} = P_{isU}).

2.3. 1st order and 2nd order maximum probe power in general condition

It has been observed for a long time that the effect of depletion can be substantially alleviated in a configuration where two probe signal waves are simultaneously present and are spectrally positioned with the same frequency interval above and below the pump pulse frequency, as depicted in Fig. 4 [14–16], one probe signal in gain configuration, the other experiencing the loss process. This spectral configuration is automatically obtained when the probe signal is generated using an intensity modulator in the simple double-sideband suppressed carrier mode [14], the lower frequency sideband with power P_{SL} and the upper sideband with power P_{SU}. It is straightforward to generalize the simple expression given by Eq. (13) to this case, by adding the contribution of the 2 probe waves in Eq. (10):

$$dP_P = -\alpha P_P(z)dz - \frac{g_B}{A_{eff}} P_P(z) P_{SL}(z) dz + \frac{g_B}{A_{eff}} P_P(z) P_{SU}(z) dz \qquad (19)$$

from which the depletion factor d can be easily determined following the same procedure:

$$1-d = e^{\frac{g_B}{A_{eff}}(P_{iSL}-P_{iSU})L_{eff}} \qquad (20)$$

where P_{iSL} and P_{iSU} are the respective input powers of the 2 probe waves at position $z = L$. This generalized expression can be indistinctively used to describe sensors operating in the gain regime (P_{iSU} = 0) or in the loss regime (P_{iSL} = 0), as well as sensors in presence of two CW probe waves equally spectrally separated from the pump.

The first order maximum CW probe signal power in the worst case situation can be easily determined by reversing Eq. (20):

$$P_{iSL} - P_{iSU} < -\ln(1-d)\frac{A_{eff}}{g_B L_{eff}} \overset{L\to\infty}{=\!=} -\ln(1-d)\frac{A_{eff}}{g_B}\alpha \qquad (21)$$

This expression shows that the system can be independent of the CW probe power and robust to the depletion when a couple of gain-loss probe signals of equal amplitude are propagating through the sensor (P_{iSL} - P_{iSU} = 0). This was soon identified as a clear merit of the double sideband configuration and it is here fully proved by this model. However, one of the probe waves must be spectrally filtered out before detection due to the opposite but equal amplitude Brillouin response of each pump-probe interaction, which consequently exactly compensate in the linear small gain approximation. Equation (21) simply expresses that the power of the 2 probe waves has no real limit and the only condition is that their power difference must not exceed the limit given for a single probe wave in Eq. (13). Practically the CW probe waves power is limited to several milliwatts by the onset of intense amplified spontaneous Brillouin scattering.

#188493 - $15.00 USD Received 8 Apr 2013; revised 25 May 2013; accepted 27 May 2013; published 4 Jun 2013

Actually this result is valid only if the amplitudes of the probe waves are negligibly modified by their interaction with the pump and the precision of the model can be improved if the contribution from this interaction on the probe waves is taken into consideration. The signal power for the 2 probe waves equally spaced from the pump can be expressed as:

$$P_{SL}(z) = P_{iSL} e^{-\alpha(L-z)} \left[1 + \frac{g_B}{A_{eff}} P_P(z) l \right] \tag{22}$$

$$P_{SU}(z) = P_{iSU} e^{-\alpha(L-z)} \left[1 - \frac{g_B}{A_{eff}} P_P(z) l \right] \tag{23}$$

where $l = V_g T / 2$ represents the interaction length over the pulse width and corresponds to the spatial resolution. The rate equation for the pump can be expressed as:

$$dP_P = -\alpha P_P(z) dz - \frac{g_B}{A_{eff}} P_P(z) P_{SL}(z) dz + \frac{g_B}{A_{eff}} P_P(z) P_{SU}(z) dz \tag{24}$$

By substituting Eq. (22)-(23) into Eq. (24), the following expression is straightforwardly obtained:

$$dP_P = -\alpha P_P(z) dz - \frac{g_B}{A_{eff}} P_P(z) \left[P_{iSL} - P_{iSU} \right] e^{-\alpha(L-z)} dz - \frac{g_B^2}{A_{eff}^2} P_P^2(z) l \left[P_{iSL} + P_{iSU} \right] e^{-\alpha(L-z)} dz \tag{25}$$

The rightmost second order term is normally much smaller than the other terms, unless $P_{iSL} \cong P_{iSU}$. It is easy to prove that, in presence of a single probe wave (P_{iSL} or P_{iSU} only), this second order term is negligible since equal to the previous first-order term multiplied by the gain during the interaction with the pump pulse, assumed to be <<1. However, if the two probe waves have equal amplitudes, the 1st order term vanishes and the effect of depletion is entirely given by this 2nd order correction.

It must be mentioned that a slight difference between P_{iSL} and P_{iSU} can lead to a compensation of the second order term by the no longer vanishing first order term [17]. This compensation is, however, exact only for a given pump power, but this power is essentially decaying while propagating along the fiber. The approach still makes sense for a partial compensation at the non-ideal expense of a careful adjustment of the relative signal powers based on a complicated setup, moreover highly dependent on the Brillouin gain distribution along the fiber.

Equation (25) does not have a simple analytical solution, but an approximate solution can be obtained by a perturbation approach, assuming that the second order term just brings a corrective factor to the first order solution given by Eq. (11). An analytical expression can be extracted if it is further assumed that the condition given by Eq. (21) is satisfied, which is not really limiting since, if not, the simple first order solution is plainly valid. Under these conditions the analytical solution including the second order correction, evaluated at the fiber far end $z = L$, can be expressed as:

$$P_P(L) = \frac{P_{iP} \, \mathrm{e}^{-\alpha L} \, \mathrm{e}^{-\frac{g_B}{A_{eff}} [P_{iSL} - P_{iSU}] L_{eff}}}{1 + \frac{g_B^2}{A_{eff}^2} P_{iP} \left[P_{iSL} + P_{iSU} \right] \mathrm{e}^{-\alpha L} \, l \, \mathrm{e}^{\frac{g_B}{\alpha A_{eff}} [P_{iSL} - P_{iSU}] \mathrm{e}^{-\alpha L}} \left\{ L - \frac{g_B}{A_{eff}} [P_{iSL} - P_{iSU}] \frac{L_{eff}}{\alpha} \right\}} \tag{26}$$

Since the denominator now contains an additive term that depends on the input pump power, the depletion with 2nd order correction is no longer independent of the pump power. The expression is quite complicated, but can be simplified considering reasonable real situations.

#188493 - $15.00 USD Received 8 Apr 2013; revised 25 May 2013; accepted 27 May 2013; published 4 Jun 2013

The numerator in Eq. (26) is the 1st order approximation as found in Eq. (11), which remains a sufficient estimation when only one probe wave is present (frequency lower or higher than the pump) and the expression Eq. (12) for the depletion remains plainly valid in this case.

Let consider hereupon the case of 2 probe waves of equal amplitude ($P_{iSL} = P_{iSU}$). The 2nd order correction must be taken into account. However, many terms vanish in Eq. (26) in this particular case, so that the pump power at the far end can be expressed as:

$$P_P(L) = \frac{P_{iP}\,\mathrm{e}^{-\alpha L}}{1+\frac{g_B^2}{A_{eff}^2}P_{iP}\,[P_{iSL}+P_{iSU}]\,\mathrm{e}^{-\alpha L}\,l\,L} \tag{27}$$

The depletion factor d can then be calculated using:

$$1-d = \frac{P_P(L)}{P_{Po}(L)} = \frac{1}{1+\frac{g_B^2}{A_{eff}^2}P_{iP}\,[P_{iSL}+P_{iSU}]\,\mathrm{e}^{-\alpha L}\,l\,L} = \frac{1}{1+G_i\,\frac{g_B}{A_{eff}}[P_{iSL}+P_{iSU}]\,\mathrm{e}^{-\alpha L}\,L} \tag{28}$$

where the expression Eq. (14) for the gain at the fiber input has been inserted. After inspecting this expression it turns out that the depletion factor d is maximum when the fiber length is exactly $L = 1/\alpha$. This can be explained as follows: the depletion naturally increases with the fiber length when the effect of attenuation is small, so for short fiber lengths. But, for longer fibers, the attenuation experienced by the signal and the pump limits the product of their power at any location along the fiber, which is the relevant quantity scaling the energy transfer between the interacting waves, as established by Eqs. (10) and (24). The distance $L = 1/\alpha$ – note this is the actual distance L and not the nonlinear effective length L_{eff} – corresponds to the intermediate situation maximizing the effect of depletion.

So, to establish for 2 equal symmetric probe waves ($P_{iSL} = P_{iSU}$) an expression similar to Eq. (13), the tolerable signal power for a given depletion d can be expressed as:

$$P_{iSL}+P_{iSU} < \frac{d}{\frac{g_B^2}{A_{eff}^2}P_{iP}\,(1-d)\,\mathrm{e}^{-\alpha L}\,l\,L} = \frac{d}{G_i\,\frac{g_B}{A_{eff}}(1-d)\,\mathrm{e}^{-\alpha L}\,L} \overset{L=1/\alpha}{<} \frac{e^1\,\alpha\,d}{G_i\,\frac{g_B}{A_{eff}}(1-d)} = \frac{e^1\,\alpha\,d\,P_{iP}\,l}{G_i^2(1-d)} \tag{29}$$

All other expressions deduced in section 2.1 can be applied in the case of 2 probe waves, in particular what concerns the error induced by a given depletion factor d.

To evaluate a typical limit value for the probe waves power, let consider the same standard conditions as in section 2.2 ($g_B = 2 \times 10^{-11}$ m/W, $A_{eff} = 80 \times 10^{-12}$ m^2, $\alpha^{-1} = 22 \times 10^3$ m), with a peak pump power $P_{ip} = 100$ mW – the maximum power before modulation instability depletes the pump [6] – and a spatial resolution $l = 1$ m, the power for each probe wave must not exceed 4.9 mW for a depletion factor $d = 0.2$. This is approximately 100X larger than for a single probe and this limit is getting even higher for longer fiber lengths. It must be pointed out that a longer spatial resolution requires a lower probe power in the exact same proportions.

This shows that a system using 2 symmetric probe waves is much more tolerant to depletion; the maximum power for the probe waves even slightly exceeds the critical power for the onset of amplified spontaneous Brillouin emission. It means the probes power will be primarily limited by this latter effect rather than depletion. This limit is valid as long as the power difference between the 2 probe waves does not exceed the limit given by Eq. (21), where the 1st order limitation remains negligible with 40 µW power difference in standard conditions.

#188493 - $15.00 USD Received 8 Apr 2013; revised 25 May 2013; accepted 27 May 2013; published 4 Jun 2013

3. Experimental validation of the model

The model presented in the previous section has been experimentally verified by a set of measurements in a uniform standard fiber. A 10 meter segment at the fiber distant end is heated locally, as illustrated in Fig. 5. The total fiber length was intentionally chosen to be relatively short – 1 km in this case – for two reasons: 1) to ensure a good uniformity of the fiber, easier to get over a short segment, so that the fluctuation of the Brillouin shift is smaller

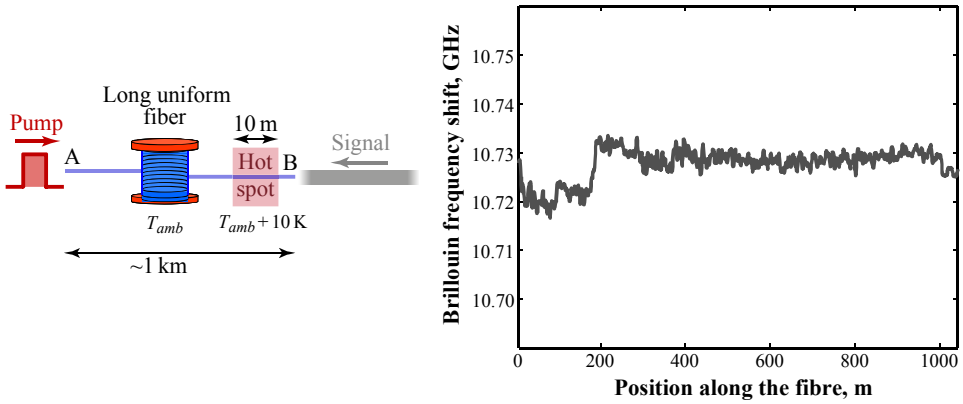

Fig. 5. Left: Experimental layout to measure the effects of depletion and to compare them with the model. A hot spot positioned near the far fiber end showing a 10 K shift in temperature is close to the worst case situation where the depletion effect are maximized. Right: Distribution of Brillouin frequency shift along the long fiber to validate its uniformity.

than the gain linewidth, and 2) to avoid large attenuation that would severely decrease the signal-to-noise ratio and would potentially screen the tiny effects due to depletion. As a result, relatively large signals have been used to make the cumulative effect of depletion visible over this short distance. These large signals are kept within the assumptions sustaining the model, so they could make the evidence of depletion effects more striking. Relatively long pump pulses have been used (50 ns) to give a high contrast gain while keeping within the small gain approximation. They also offer the crucial advantage to induce a very minor broadening on the effective gain spectrum to preserve its native Lorentzian shape. The pulses were shaped using a semiconductor optical amplifier operating in gated mode, so that an effective on/off ratio higher than 55 dB was achieved, making any biasing effect due to a continuous baseline fully negligible since satisfying by a margin of 2 orders of magnitude the condition given by Eq. (18). Figure 5 also shows the distribution of the peak Brillouin gain frequency along the fiber, which is slightly non-uniform over the first 200 m that corresponds to a layer on the fiber drum spooled with a smaller tension. This offset remains smaller than the Brillouin gain linewidth and probably explains the small systematic deviations between the model and measurements.

3.1. Measurements of the amount of depletion

Using a classical BOTDA technique with a single probe wave in a gain configuration the

#188493 - $15.00 USD Received 8 Apr 2013; revised 25 May 2013; accepted 27 May 2013; published 4 Jun 2013

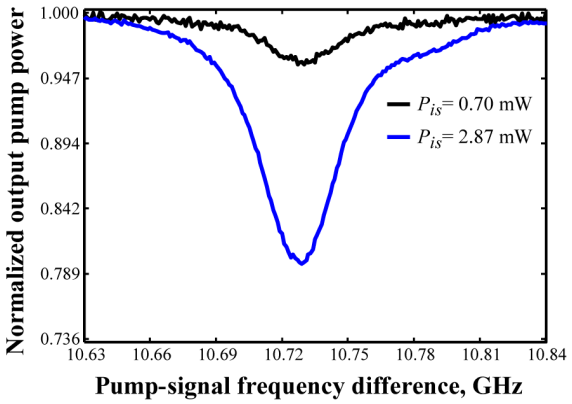

Fig. 6. Output pump pulse peak power as a function of the frequency difference between pump and signal for two different values of the signal input power P_{is}.

pump depletion was first evaluated by measuring the relative peak power of the pump pulse at the fiber output while scanning the frequency difference between pump and probe. This relative pump power is graphed in Fig. 6 for 2 different probe powers, showing the substantial power drop at the center of the Brillouin gain. This kind of measurement is a simple and direct quantitative measurement of the depletion factor *d*. The measurement is scaled by normalizing the output pump power at the peak gain frequency to its off-gain value, obtained far from the gain central frequency. Figure 7 (left) represents the measured depletion factor *d* for various probe powers, where the solid curve is the prediction obtained using Eq. (12). The experimental values are only slightly smaller than the prediction and the discrepancy can be explained by the residual non-uniformity along the fiber and the gain spectral offset between the hot spot and the long uniform segment, which is not exactly ideal to maximize the error. Figure 7 (right) represents the depletion factor *d* for a varying pump power while keeping the probe power constant. The depletion does not change while the gain experienced by the probe is very substantially modified. This experimentally confirms the remarkable fact that the depletion is independent of the pump power in a first-order small gain approximation.

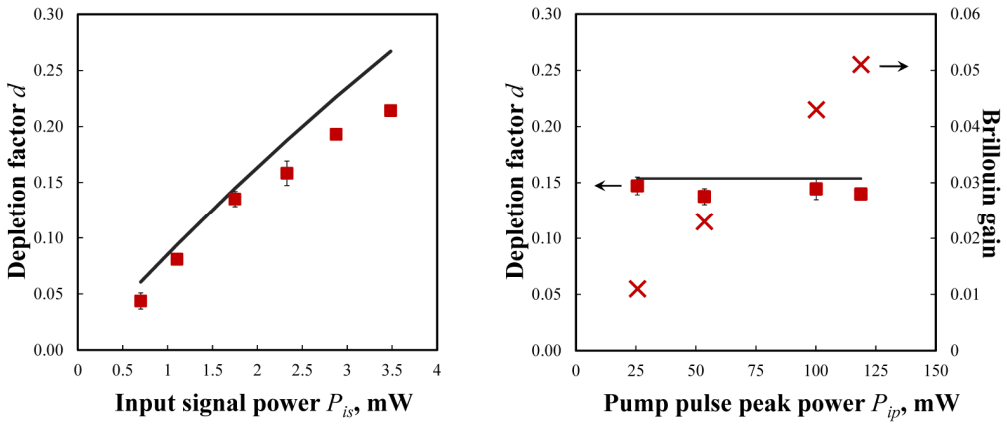

Fig. 7. Left: Depletion factor *d* as a function of the input power of the CW signal, for a fixed input pump peak power P_{ip} of 70 mW. Red squares are experimental points with error bars, while the solid black line is the model prediction. Right: Depletion factor *d* as a function of the input pump peak power of the, for a fixed input power of the CW signal P_{is} = 1.91 mW. Red squares are experimental points with error bars, while the solid black line is the model prediction. The pump power has no impact on the amount of depletion, while it changes the signal gain linearly (red crosses).

#188493 - $15.00 USD Received 8 Apr 2013; revised 25 May 2013; accepted 27 May 2013; published 4 Jun 2013

The same set of measurements was carried out using a double probe wave configuration, symmetrically spectrally positioned, so that one wave is experiencing a gain process while the other is subject to a loss process, as shown in Fig. 4. As a function of the pump-probe frequency difference, the output pump power is shown in Fig. 8, for various probe powers. It must be pointed out that the probes power is substantially higher than that in the measurement shown in Fig. 6, while the depletion is fairly smaller on a comparable scale. The experimental spectra are entirely different to those using a single probe wave. The output power spectral distribution seems mainly following the derivative of the gain spectrum. This feature can be easily explained by the fact that the gain and loss spectra are not perfectly superposed or, in other words, the peak gain frequencies are not exactly identical for the 2 symmetrically positioned probe waves. This results from the fact that the Brillouin frequency shift only depends on the frequency of the interacting wave of higher energy and these waves are distinct in the present combined process (pump for the gain process on the lower frequency probe wave, high frequency probe wave for the loss process on the same probe wave). A straightforward calculation shows that the mismatch between the peak gain frequencies is equal to:

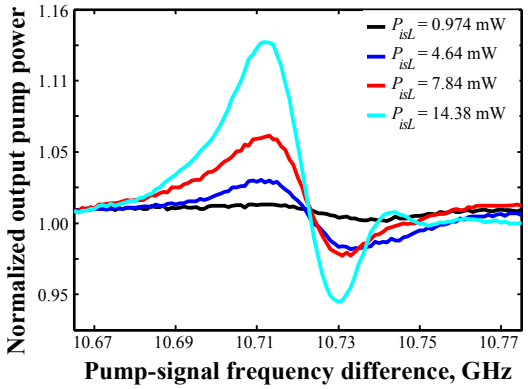

Fig. 8. Output pump pulse peak power as a function of the frequency difference between pump and signal in the double probe wave configuration, for 4 different values of the input power P_{isL} of one of the signals. The 2 signals show very identical powers.

$$\delta f = 2\frac{nV_a}{c}(\nu_P + \nu_B) - 2\frac{nV_a}{c}\nu_P = 2\frac{nV_a}{c}\nu_B = \frac{\nu_B^2}{\nu_P} \tag{30}$$

which is about 600 Hz in a standard fiber at λ = 1550 nm. This tiny difference makes a full compensation by gain and loss at all frequencies impossible and explains the derivative aspect of the depletion spectral dependence in Fig. 8. For a complete compensation at all frequencies, the 2 probe waves must be slightly asymmetrically positioned with respect to the pump wave, by some ½ × 600 = 300 Hz. The more pronounced asymmetry observed for high probe powers is a direct consequence of the large pump gain-loss integrated all over the fiber in this situation, so that the small gain linear approximation no longer holds and the asymmetry results from the exponential dependence of the pump gain-loss on the probe power.

To evaluate the depletion factor *d* from these measurements, the peak excursion of the output pump power from the off-gain value was considered, which is not necessarily corresponding to the peak gain frequency but is representation of the worst case situation. The experimental

#188493 - $15.00 USD Received 8 Apr 2013; revised 25 May 2013; accepted 27 May 2013; published 4 Jun 2013

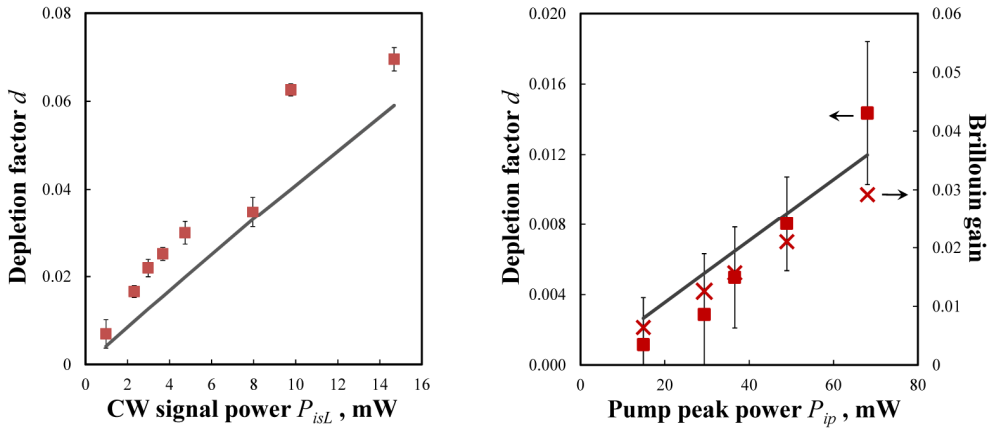

Fig. 9. Left: Depletion factor d in the double probe wave configuration as a function of the input power of the one of the CW signals, for a fixed input pump peak power P_{ip} of 60 mW. Red squares are experimental points with error bars, the solid black line is the model prediction. Right: Depletion factor d as a function of the input pump peak power of the, for a fixed input power of one of the CW signal P_{isL} = 2.48 mW. Red squares are experimental points with error bars, while the solid black line is the model prediction. The pump power has a slight impact on the amount of depletion, while it keeps changing the signal gain linearly (red crosses).

depletion factor d is graphed as a function of the probe powers in Fig. 9 (left). The solid line corresponds to the estimated values from Eq. (26), which slightly underestimates the real depletion as a result of the peak gain frequency mismatch. It must be pointed out that depletion in this case is much smaller than in the case of a single probe wave, while the signal waves power is much higher. The difference can be observed by comparing Fig. 7 (left) and Fig. 9 (left). The 2 signal waves were synthesized from the pump source using the sidebands generated by an intensity electro-optic modulator in a suppressed carrier configuration, so that they were automatically symmetrically positioned. The residual phase modulation in the modulator resulted in 2.2% power difference in the two sidebands. Due to this difference, the complete Eq. (26) was used instead of the simplified Eq. (28) for the estimation of depletion in Fig. 9 (left). Equation (26) also predicts a small dependence on the peak pump power P_{ip} for the depletion factor d, that is confirmed by the measurement shown in Fig. 9 (right), in excellent agreement with the model.

3.2. Measurement of the frequency error as a function of depletion

Returning to the scheme shown in Fig. 5, the short 10 m segment was heated to shift the Brillouin gain spectrum along this segment with respect to the long uniform preceding fiber. The temperature difference between the short segment and the long fiber was 10 K, so that the condition for a maximum depletion effect given by Eq. (7) is closely realized. Figure 10 shows the measured local Brillouin gain spectrum at the center of the short segment, for different probe powers and for a fixed peak pump power of 69 mW. The measurements have been carried out in the single probe wave gain configuration, for which the impact of depletion is crucial. The pump was launched at end A in Fig. 5, so that it fully experiences the cumulative effect of depletion along the long uniform fiber. A reference spectrum was then measured by launching the pump at end B – realized by swapping the fiber ends in the system, in which case the pump depletion is totally negligible at the heated segment location. This reference spectrum is also shown in Fig. 10 for comparison, clearly emphasizing the skewing effect on the measured gain spectrum due to pump depletion.

This biasing effect is fully confirmed by evaluating the peak gain frequency as a function of position in the short segment, as shown in Fig. 11. The difference in the evaluated

#188493 - $15.00 USD Received 8 Apr 2013; revised 25 May 2013; accepted 27 May 2013; published 4 Jun 2013

Brillouin frequency shift is absolutely striking when comparing the values obtained for a segment placed at the far end (pump launched at end A) with those obtained for a segment placed at the near end (pump launched at end B). The detrimental effect of an increasing signal power is also clearly demonstrated.

The quantitative validity of the model is also tested by comparing the experimental error ν_e on the evaluated Brillouin frequency shifts to that predicted by the model using Eq. (6), as a function of the actual measured depletion d. This comparison is shown in Fig. 12. The excellent agreement gives a solid confidence in the robustness of the model.

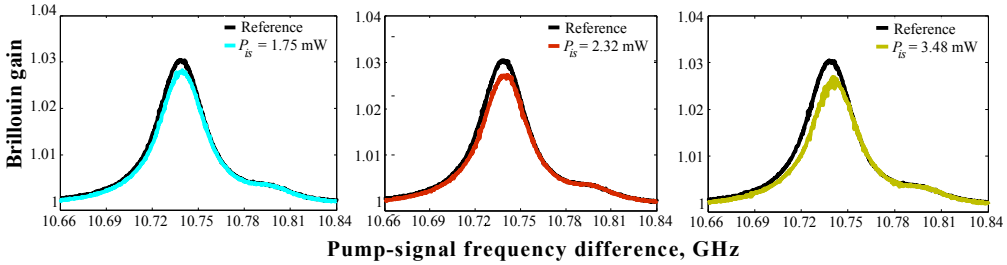

Fig. 10. Brillouin gain spectrum measured within the 10 m hot spot described in Fig. 5 when its temperature is shifted by 10 K, for different powers of the CW signal and for a fixed pump peak power of 69 mW. The colored curves are obtained when the hot spot is placed at the far end, while the black reference curves are for a hot spot placed at the near end. This clearly shows the skewed distortion of the gain spectrum.

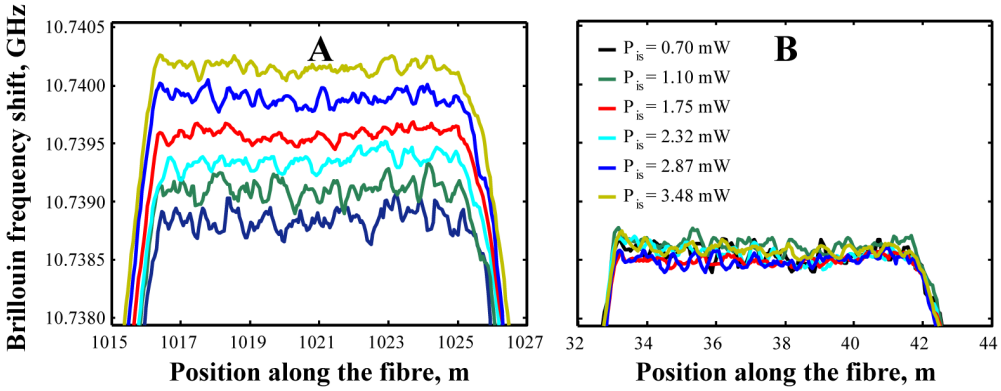

Fig. 11. Brillouin frequency shift as function of the position along the hot spot, for different power P_{is} of the CW signal. In case A, the hot spot is placed at the far end (see Fig. 5) and the strongest biasing effect of depletion is experienced, while in case B, the hot spot is placed at the near end where the pump has not yet accumulated any depletion and the measured Brillouin frequency shift is identical for all probe powers.

#188493 - $15.00 USD Received 8 Apr 2013; revised 25 May 2013; accepted 27 May 2013; published 4 Jun 2013

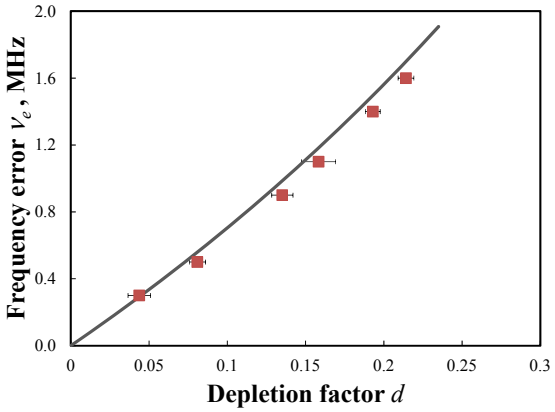

Fig. 12. Measured frequency error as a function of the measured depletion factor d (red squares) in the worst case experimental situation depicted in Fig. 2 & 5. The black curve is obtained from the model using Eq. (8) for $\delta\nu = 10$ MHz.

4. Discussion and conclusion

A model has been developed and completed to evaluate the cause and limitations of the depletion effect in BOTDA sensors. All experimental results are consistent with this model, strikingly demonstrating the detrimental effect of depletion that has been neglected to a wide extent in former reports from different research teams. The model suggests two guidelines for designing a distributed Brillouin sensor that is robust to depletion. The probe signal power must be kept as low as possible while the pump pulse power can be freely increased up to the limit given by other nonlinear effects [6], since the depletion is independent of the pump power to the first order and highly dependent on the probe power. This criterion indicates that all configurations based on an intense CW probe signal and a weak pump pulse are essentially mined by depletion. In the meantime, the robustness to depletion can be significantly improved by adopting a double-sideband configuration, in which no practical limit is observed up to a level close to the onset of the amplified spontaneous Brillouin emission. These guidelines show that the depletion can be fully controlled and avoided by a proper design without other changes on the sensing fibers. Some recently proposed configurations segmenting the sensing fiber in sections showing different Brillouin gain spectra [18] or by a time multiplexing scheme [19, 20] make sense only if they effectively lead to a substantial decrease of the nonlinear effective length L_{eff} that is the distance scaling quantity for depletion. This means that each segment must be fairly shorter than the asymptotic effective length of ~22 km and segmenting the fiber in sections longer than this asymptotic effective length is essentially useless.

The robustness of a BOTDA system to depletion can be simply tested and should be normally proved in the future when given accuracies and performances are claimed. This can be realized by implementing a configuration similar to Fig. 5, by using a long uniform sensing fiber of length equivalent to the claimed distance range. By evaluating the amount of depletion on the output pump power (see Fig. 6) and comparing it with the value given by Eq. (8) or deduced from the graph shown in Fig. 3, it can be easily determined if the systematic error due to depletion is smaller than the claimed or measured accuracy. It must be stressed that in no way the biasing effect due to depletion can be estimated by repeating measurements in the same configuration and evaluating their standard deviation, because it is a systematic repeatable error.

A more solid test giving a full experimental evaluation of the error ν_e on the Brillouin frequency shift can be implemented by using a long uniform fiber having a length equivalent to the claimed distance range. The Brillouin frequency at the far end of this fiber is shifted by

#188493 - $15.00 USD Received 8 Apr 2013; revised 25 May 2013; accepted 27 May 2013; published 4 Jun 2013

locally modifying the temperature or the applied strain over a short section, albeit longer than the spatial resolution. The amount of shift must be $\delta\nu = \Delta\nu/4$ and the measured Brillouin shift must correspond to the real value that can be obtained by measuring the short segment only. This can be actually realized using the procedure described in Section 3.2 to obtain the measurements shown in Fig. 11.

These conclusions show that the depletion is a valid limitation in current configurations. The depletion has non-negligible impact but it can be fully controlled and made negligible by an intelligent sensor design.

Acknowledgments

The authors address their warm thanks to Prof. Moshe Tur from Tel Aviv University and to Prof. Miguel Gonzalez Herraez from University of Alcala-Madrid for their critical points of view, crucially helpful for the proper development of this model. This study was realized in the framework of the European COST Actions 299 "FIDES" and TD1001 "OFSeSa", supported by the project C06.0015 and C10.0093 from the Swiss State Secretariat for Education, Research and Innovation.

#188493 - $15.00 USD Received 8 Apr 2013; revised 25 May 2013; accepted 27 May 2013; published 4 Jun 2013